APL Materials

Polarization controlled photovoltaic and self-powered photodetector characteristics in Pb-free ferroelectric thin film

Cite as: APL Mater. **7**, 011106 (2019); https://doi.org/10.1063/1.5064454
Submitted: 04 October 2018 • Accepted: 28 December 2018 • Published Online: 24 January 2019

Atal Bihari Swain, Martando Rath, Pranab Parimal Biswas, et al.

Polarization controlled photovoltaic and self-powered photodetector characteristics in Pb-free ferroelectric thin film

Cite as: APL Mater. 7, 011106 (2019); doi: 10.1063/1.5064454
Submitted: 4 October 2018 • Accepted: 28 December 2018 •
Published Online: 24 January 2019

Atal Bihari Swain,[1] Martando Rath,[1,2] Pranab Parimal Biswas,[1] M. S. Ramachandra Rao,[1,2] and P. Murugavel[1,a)]

AFFILIATIONS

[1] Department of Physics, Indian Institute of Technology Madras, Chennai 600036, India
[2] Nano Functional Materials Technology Centre, Department of Physics, Indian Institute of Technology Madras, Chennai 600036, Tamil Nadu, India

[a)] **Author to whom correspondence should be addressed:** muruga@iitm.ac.in

ABSTRACT

Ferroelectrics are considered next generation photovoltaic (PV) materials. In this work, a switchable and large PV effect is demonstrated in a Pb-free ferroelectric $0.5Ba(Zr_{0.2}Ti_{0.8})O_3$-$0.5(Ba_{0.7}Ca_{0.3})TiO_3$ (BZT-BCT) thin film fabricated by a pulsed laser deposition technique. The material shows a remarkable PV output of 0.81 V due to its morphotropic phase boundary composition. The observed PV effect is analyzed on the basis of the interfacial Schottky barrier and bulk depolarization field. The poling dependent PV studies revealed that although the Schottky and depolarization field contribute to the PV effect, the latter dominates the PV response beyond the coercive field. Additionally, the importance of this compound in the field of a self-biased photodetector is elucidated in terms of calculated photodetector parameters such as responsivity and detectivity. The explored results will bring significant advancement in the field of ferroelectric PV, UV solid state detector applications and also give an additional dimension to the multifunctional ability of the BZT-BCT system.

Ferroelectric materials showing switchable spontaneous polarization offer intriguing research interest due to their application potentials in a wide range of fields.[1–5] Recently, the photovoltaic (PV) research on ferroelectrics is gaining momentum because of anomalous PV response.[6–10] However, these studies are confined to a few ferroelectric systems such as $LiNbO_3$,[6] $BaTiO_3$,[6–8] $(Pb_{0.97}La_{0.03})(Zr_{0.52}Ti_{0.48})O_3$,[9] $PbTiO_3$,[10] $BiFeO_3$ (BFO),[11–16] and $Pb(Zr_{1-x}Ti_x)O_3$ (PZT)[17–20] in the literature. Some of these perovskite oxides are discovered to yield giant PV response but mostly in their bulk form.[6–10] Glass *et al.*[21] reported the generation of open circuit electric field (E_{OC}) as high as 10^5 V/cm in an Fe doped $LiNbO_3$ single crystal. In fact, the recent studies on BFO, $Ba_{1-x}(Bi_{0.5}Li_{0.5})_xTiO_3$ have showed giant PV response in these systems.[16,22] However, the origin of the ferroelectric PV effect is not clearly understood and the proposed mechanisms vary from the bulk to the thin film.[2,23] The above bandgap photovoltage in ferroelectrics known as bulk PV effect (BPVE) is associated with shift current mechanism due to non-centrosymmetry of the system.[24–27] On the other hand, the domain wall, the interface, and the associated phenomena could play a critical role in the PV effect observed in thin film heterostructures.[2,11,28] In fact, the electrode dependent photo-current response reported in the PZT thin film suggests that the PV mechanism in thin films is different from the anomalous PV effect in the ferroelectric bulk and single crystals.[20] In this context, understanding the PV effect in thin films is essential to enhance their application potentials in the era of miniaturization.

In thin films, the domain wall theory is proposed to explain the observed above-bandgap voltages in the epitaxial $BiFeO_3$ film.[11] The theory suggests that the cumulative effect of electrostatic potential at ferroelectric domain walls is the driving force for the charge carrier separation.[11]

Subsequently, the temperature dependent PV measurements carried out on the epitaxial $BiFeO_3$ film clarified the significant role played by BPVE than the domain wall theory.[29,15] Alternatively, the interface related Schottky junction effect is proposed to control the PV effect in thin film metal-ferroelectric heterostructures.[19,20,28,30] The effect of the Schottky barrier at the metal-ferroelectric interface and its modulation by the polarization induced controllable charge carrier injection on the PV response are discussed in $SrRuO_3$(SRO)/PZT/SRO and Pt/BFO/SRO thin films.[18,28] The photocurrent response with poling voltage mimicking the polarization hysteresis loop indeed suggests the polarization effect on the PV response.[18,28] In addition, the role of the internal electric field induced imprint effect on photo-current response in the epitaxial PZT film is demonstrated in the literature.[19] However, the dominance of the interfacial Schottky junction over polarization field and vice versa is not clearly elucidated in the literature. Moreover, to optimize the performance of the ferroelectric based PV devices, it is necessary to understand the competition between these mechanisms at the interface.

Apart from energy harvesting applications of ferroelectrics, their bandgap aiding UV light absorption foresees their application prospective in UV solid state detectors.[5,31] The traditional UV photodetectors made of wide bandgap semiconductors (ZnO, SnO_2, TiO_2, ZnS, GaN, SiC, etc.)[32–34] require an external bias for charge separation which restricts their suitability for miniaturization and integration of devices. In this context, the perovskite ferroelectrics showing large photo-response can be an ideal self-powered (zero-bias field) photodetector due to its in-built polarization field facilitating the charge separation.[5,35]

Among the existing ferroelectrics, the recently discovered $0.5Ba(Zr_{0.2}Ti_{0.8})O_3$-$0.5(Ba_{0.7}Ca_{0.3})TiO_3$ (BZT-BCT)[36] compound exhibiting outstanding piezoelectric properties with a large piezocoefficient (d_{33} ~ 620 pC/N) is considered as an alternative to Pb-based piezoelectric systems. Furthermore, it also attracts tremendous research interest due to its multifunctional ability with the large energy storage density,[37] better electrocaloric effect,[38] highest electro-optic[39] properties, etc. Additionally, the BZT-BCT composition exhibiting the morphotropic phase boundary (MPB) is expected to yield large photo-response because of its suitable symmetry requirements.[9,40] Hence, it is highly imperative to investigate the PV and photodetector studies on this technologically important BZT-BCT material. In this work, the polycrystalline BZT-BCT thin film fabricated on the Pt/TiO_2/SiO_2/Si substrate revealed a remarkable PV response with a maximum open circuit voltage (V_{OC}) of 0.81 V, which is higher than the value reported for few ferroelectric polycrystalline films.[41,42] The poling dependent PV studies elucidate the dominance of polarization effect over the interfacial Schottky barrier effect at poling fields higher than the coercive field. In addition, the UV photodetector characteristics of the BZT-BCT sample are demonstrated in this work.

Polycrystalline BZT-BCT films were deposited on Pt/TiO_2/SiO_2/Si substrates using a pulsed laser deposition (PLD) technique. Prior to deposition, the BCT-BZT compound was prepared by the conventional solid state route by mixing stoichiometric amounts of $BaCO_3$, $CaCO_3$, $BaZrO_3$, and TiO_2 precursors and calcining the homogeneous mixture at 1350 °C for 4 h. The BCT-BZT target of 12 mm diameter prepared from the calcined powder was sintered at 1450 °C for 6 h. The film was deposited on the substrate maintained at 720 °C by ablating the target for 20 min under 400 mTorr oxygen partial pressure (PO_2). After deposition, the film was *in situ* annealed under 400 Torr of PO_2 for 30 min and then cooled to room temperature at 10 °C/min. The grown film was again subjected to *ex-situ* annealing under the ambient atmosphere at 850 °C for 1 h for better crystallinity.

The fabricated film was characterised by X-ray diffraction (XRD), using a Rigaku diffractometer fitted with a Ni filter and Cu K_α radiation, for phase confirmation. The thickness of the sample was measured by performing cross-sectional imaging using an Inspect F50 field emission scanning electron microscope (FESEM). The optical bandgap of the film was obtained using diffuse reflectance spectroscopy (DRS) by employing a micropack DH2000 lamp (deuterium in UV-vis and Halogen in vis-NIR). For electrical measurements, semi-transparent Au dots of 500 μm diameter and 18 nm thickness were deposited by thermal evaporation technique and are used as top electrodes. The polarization switching studies were carried out on Au/BZT-BCT/Pt capacitor geometry using a Radiant Technology instrument (USA RT6000S). Ferroelectric domain switching was performed using a piezoresponse force microscopy (PFM) (*Parks System* XE, USA). The conducting Au tip with a resonant frequency of 75 kHz and a force constant of 2.5 N/m was used for PFM studies. The PV responses were recorded using a Keithley high resistance electrometer (6517B) with a xenon arc lamp as the light source.

The XRD patterns recorded on the BZT-BCT/Pt/TiO_2/SiO_2/Si sample and the substrate are shown in Fig. 1(a). The sample XRD pattern reveals that the film is grown in phase pure polycrystalline form without any secondary phases. The diffraction peaks are indexed to the tetragonal symmetry of the BZT-BCT compound. The cross-sectional SEM image shown in Fig. 1(b) confirms the uniform deposition of the film on the substrate with a homogeneous thickness of around 700 nm. To obtain the optical bandgap, the percentage of reflectance (R%) is recorded as a function of wavelength and it is plotted in Fig. 1(c) from 325 to 800 nm. The inset shows the Kubelka-Munk (K-M) plot which is a plot of $(F(R)h\nu)^{1/2}$ versus energy, where F(R) is the K-M coefficient ($(1 - R)^2/2R$), R is the reflectance, and hν is the photon energy.[43] The optical bandgap extracted from the linear fitting of the K-M plot is around 3.2 eV, which falls in the UV-visible region of the solar spectrum.

Prior to the ferroelectric measurements, the fabricated film is tested for its leakage characteristics and the current density is plotted as a function of the applied electric field in Fig. 1(d). The plot displays that the leakage current density (J) is of the order of 10^{-7} A/cm^2, which is a typical range observed for ferroelectric materials. As a consequence, the polarization (P) response to the applied electric field (E) shown in Fig. 1(e)

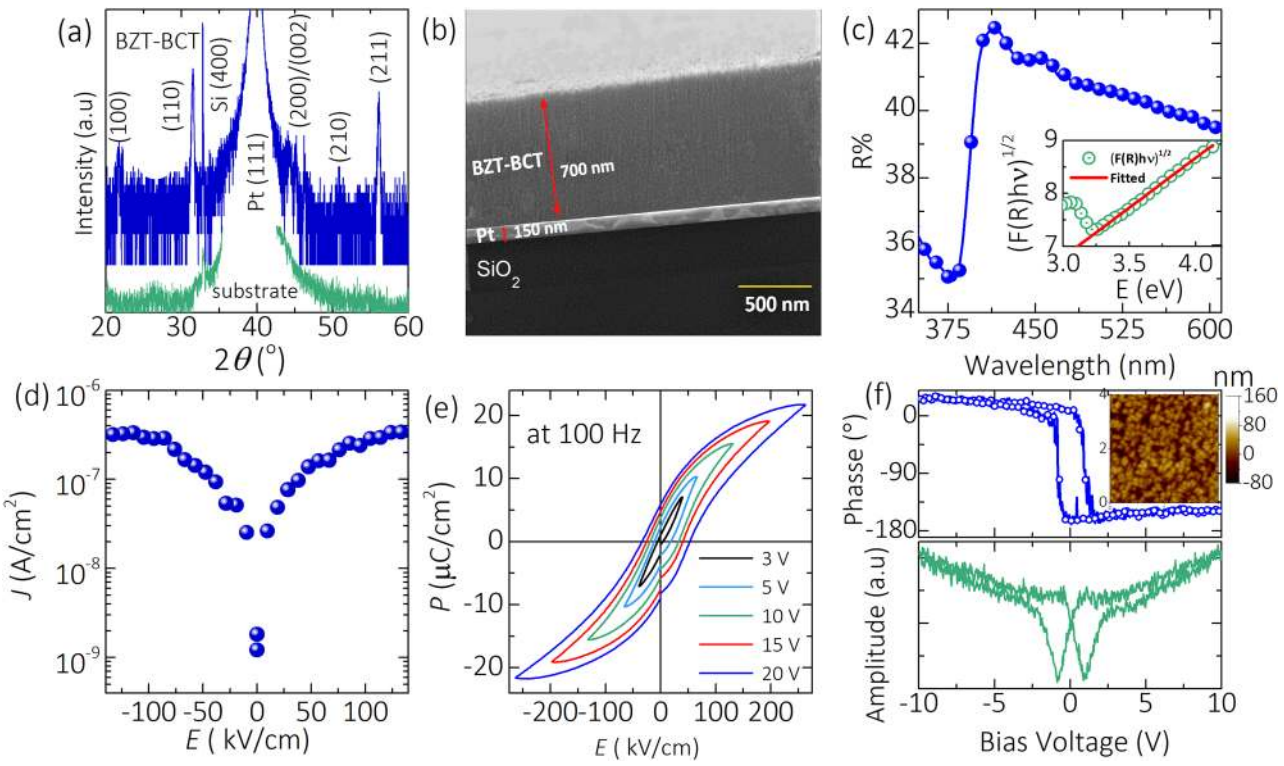

FIG. 1. (a) XRD pattern of the BZT-BCT film and the Pt/TiO_2/SiO_2/Si substrate, (b) the cross-sectional SEM image of the BZT-BCT film showing 700 nm thickness, and (c) R% versus wavelength recorded on the film (the inset shows the respective K-M plot). (d) Leakage current density versus applied electric field, (e) the *P-E* hysteresis loop measured at a different maximum applied electric field range, and (f) the PFM phase and amplitude response of the domains as a function of bias voltage for the BZT-BCT film. The inset shows the AFM topographic image of the as-grown film.

gives a P-E hysteresis loop behavior with a maximum polarization of 22 $\mu C/cm^2$ at 240 kV/cm. The evolution of the P-E loop at a different maximum applied field range is well demonstrated in Fig. 1(e). The small voltage off-set seen in the coercive field ($E_{coercive}$) is due to the use of asymmetric electrodes. The $E_{coercive}$ inferred from the P-E loop obtained at ±20 V sweep is 62.4 kV/cm (4.2 V). To ascertain the domain switching characteristics of the film, the phase and amplitude responses of the domains as a function of dc bias voltage are probed by PFM and the resultant plots are given in Fig. 1(f). The topographic image over $4 \times 4\ \mu m^2$ area of the BZT-BCT film shown in the inset of Fig. 1(f) indicates that the film is grown with smooth surface. The average surface roughness of the film is ~5 nm. The phase curve reveals 180° domain switching, and the saturated butterfly loop displayed by the amplitude curve reiterates the ferroelectric nature of the film. The observed bandgap along with good ferroelectric characteristics of the BZT-BCT film having MPB composition strongly suggests its possibility to show large photo-response.[9,36]

To investigate the PV effect, the photo-response measurements are carried out on the Au/BZT-BCT/Pt sample using a 100 mW/cm^2 intensity xenon-arc lamp light source. The schematic diagram representing the measurement geometry is shown in Fig. 2(a). Since the photo-response is expected to be proportional to the polarization of the material, the sample is poled under an external voltage of 6 V (which is well above the $E_{coercive}$ of the Au/BZT-BCT/Pt capacitor) for 600 s. The bottom (Pt) and the top (Au) electrodes are connected to the positive and negative terminals, respectively, and the resultant polarization state is labeled the UP-poled state. The measured photovoltaic J-V characteristics under dark and light illumination conditions are shown in Fig. 2(b). From this figure, it is inferred that the sample shows the maximum V_{OC} of 0.81 V with a short-circuit current density (Jsc) of ~−36 $\mu A/cm^2$. Note that the observed V_{OC} is larger than the reported values for well-studied pure $BiFeO_3$ films.[14,41,42]

The ferroelectric film is expected to show PV switchability by altering the direction of polarization.[12,13,28] This effect is examined in the Au/BZT-BCT/Pt film after subjecting it to the DOWN-poled state by applying 6 V for 600 s (the bottom and top electrodes are connected to the negative and positive terminals, respectively). The resultant J-V curves measured under dark and light illumination conditions, shown in Fig. 2(b), indeed confirm the switchable PV characteristics, a typical behavior of a ferroelectric PV cell with V_{OC} ~ −0.79 V and J_{SC} = 25 $\mu A/cm^2$.

To study the transient current response to light, the time dependent J_{SC} is measured under light ON and OFF conditions

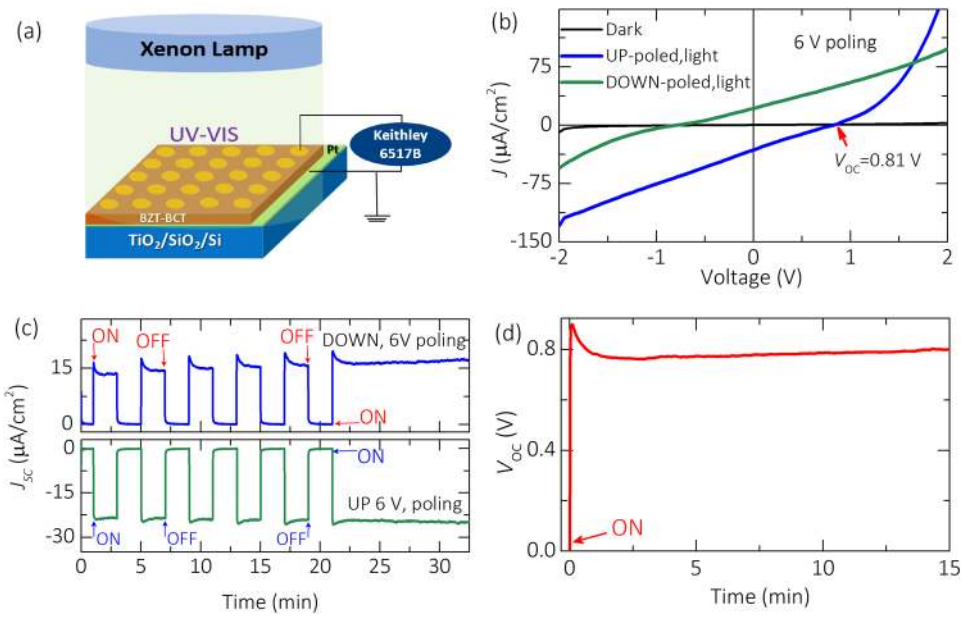

FIG. 2. (a) Schematic diagram representing the PV measurement geometry, (b) *J-V* characteristics for UP/DOWN 6 V poled under dark and light illumination conditions, (c) photo-current response with light ON and OFF state, and (d) V_{OC} stability with light illumination time for the BZT-BCT film.

for both UP- and DOWN-poled states of the sample and the results are plotted in Fig. 2(c). The J_{SC} shows a sharp response under light ON and OFF conditions with an initial spike-like structure, followed by the steady state current. The initial spike-like feature is attributed to the pyroelectric response of the ferroelectric sample which is a common feature observed in ferroelectrics under light illumination.[25] The small variation in magnitude of J_{SC} observed between the UP- and DOWN-poled states [Fig. 2(c)] can be correlated with the asymmetric electrode effect.[12] The stability of the generated photocurrent is confirmed by measuring the J_{SC} under the light ON state for a longer duration, as shown in Fig. 2(c). Similarly, the stability of V_{OC} under the light ON state is verified by measuring the V_{OC} for a longer duration and the result is plotted in Fig. 2(d).

Interestingly, the observed J-V curve under light illumination shows the predominant linear behavior [see Fig. 2(b)], which is the reminiscent effect of the ferroelectric depolarization field. However, in a metal-ferroelectric-metal heterostructure, the I-V characteristic can be significantly modulated by two major mechanisms, the interfacial and the bulk controlled mechanism.[30] The former is attributed to the effect of interface control by charge injection due to the Schottky effect, and the latter is attributed to the contributions from Ohmic, space charge limited currents, depolarization field, or their combinations. Figure 3(a) depicts the schematic representations of I-V curves originating from these contributions. In a metal-semiconductor contact, the difference in metal work-function and semiconductor electron affinity gives rise to a barrier at the interface,[30,44–46] as predicted by

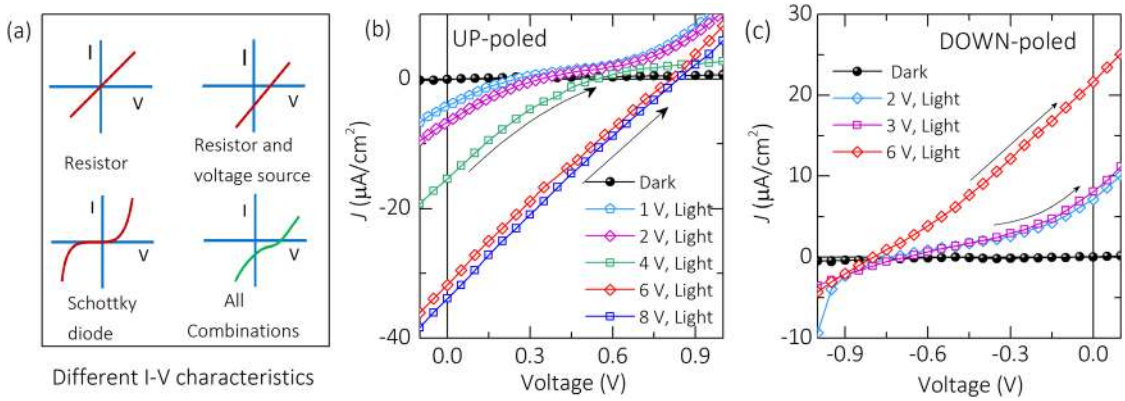

FIG. 3. Schematic diagrams representing the *I-V* characteristics of (a) resistor, resistor and voltage source, Schottky diode, and their combinations. Photovoltaic *J-V* characteristics for (b) UP-poled and (c) DOWN-poled state of the BZT-BCT film recorded under dark and light illumination conditions.

the Schottky-Mott rule. The smaller Schottky barrier height (φ), in comparison with the thermal energy, gives a linear I-V curve passing through zero, as shown in Fig. 3(a) (resistor nature), which indicates the Ohmic or resistive nature of the interface.[44] Although the I-V is linear for the combination of interfacial Ohmic and the bulk capacitive nature of the material, it will make an intercept at the voltage and current axes, as shown in Fig. 3(a) (resistor and voltage source).[15,29,47] However, at sufficiently larger φ, the semiconductor-metal interface will be depleted and behaves as a Schottky diode with a typical I-V curve, as shown in Fig. 3(a) (Schottky diode).[45]

It is known that perovskite oxide ferroelectrics are generally termed semiconductors and charge carriers are introduced by the defect chemistry and unavoidable oxygen vacancies. Therefore, in the metal/ferroelectric interface, both the interfacial Schottky barrier and bulk contributions due to polarization could play a role in the observed PV response and hence may give I-V characteristics, as shown in Fig. 3(a) (combined effect). As a result, the observed photo-response for the BZT-BCT film shown in Fig. 2(b) is the coupled phenomena of the bulk polarization and the interfacial Schottky barrier effect. However, the predominant linear nature of the J-V curve[24,41,47] strongly suggests that the polarization contribution to the PV response is dominant over the interfacial Schottky contribution.

To probe the competing role of the interfacial Schottky and bulk polarization effect, systematic poling dependent PV studies are carried out. For this purpose, the sample is UP-poled at 1, 2, 4, 6, and 8 V and the PV measurements are carried out under dark and light illumination conditions. The recorded J-V characteristics are shown in Fig. 3(b). Interestingly, the J-V curves display two distinctly different features appearing at two different poling field ranges. The non-linearity in J-V curves (as guided by arrow heads) in Fig. 3(b) at lower poling fields, from 1 to 4 V, reveals a Schottky-like behavior, and it indicates the dominant interfacial Schottky effect in the PV response. However, at higher poling fields, from 6 to 8 V, the J-V curves show the predominant linear features (highlighted by an arrow) and they indicate the dominant bulk polarization effect in the PV response. The J-V characteristics show similar features for the sample subjected to the DOWN-poled state, as shown in Fig. 3(c).

To explain the poling field (E_{poled}) dependent PV response in the ferroelectric Au/BZT-BCT/Pt film, the schematic energy band diagrams are drawn in Fig. 4. Generally the ferroelectric BZT-BCT film is considered an n-type semiconductor due to the inherent nature of perovskite oxides having oxygen vacancies and the possible mixed valence state of the Zr/Ti metal ions (generated to maintain the overall charge neutrality of the system) acting as electron donors.[30,45,48] Hence, the BZT-BCT and Au/Pt contacts facilitate the formation of Schottky barriers at the top and bottom electrode interfaces due to band bending so as to match the metal and semiconductor Fermi levels (E_F). The corresponding schematic band diagram illustrating the band bending mechanism, giving the built-in-potential ($\varphi_{bi} = \varphi_b - \varphi_t$) at the interface and the associated built-in-field[35] $E_{bi} = \varphi_{bi}/(q \times d)$, for an unpoled sample is drawn in Fig. 4(a). Here, φ_t and φ_b are the barrier heights at the top and bottom electrode/film interfaces, respectively, q is the charge, and d is the thickness of the film. Note that E_{bi} at the metal-semiconductor interface facilitates the separation of photo-generated carriers.[20] However, the barrier potential could be modified (φ'_{bi}) by E_{poled}. As a result, the sample subjected to the poled state shows that the net internal field ($E_{net} = E_{bi} \pm E_{dp}$) is the combination of the Schottky (E_{bi}) and depolarization field (E_{dp}).[14,26,41] When $E_{poled} < E_{coercive}$, the observed Schottky-like non-linearity in J-V curves under light illumination [Fig. 3(b)] suggests that $E_{bi} \geq E_{dp}$. On the other hand, when $E_{poled} > E_{coercive}$, the observed predominant linear J-V curves under light illumination [Fig. 3(b)] suggests that $E_{bi} < E_{dp}$. Overall, these poling dependent J-V characteristic features of the BZT-BCT sample can be understood from Figs. 4(b)

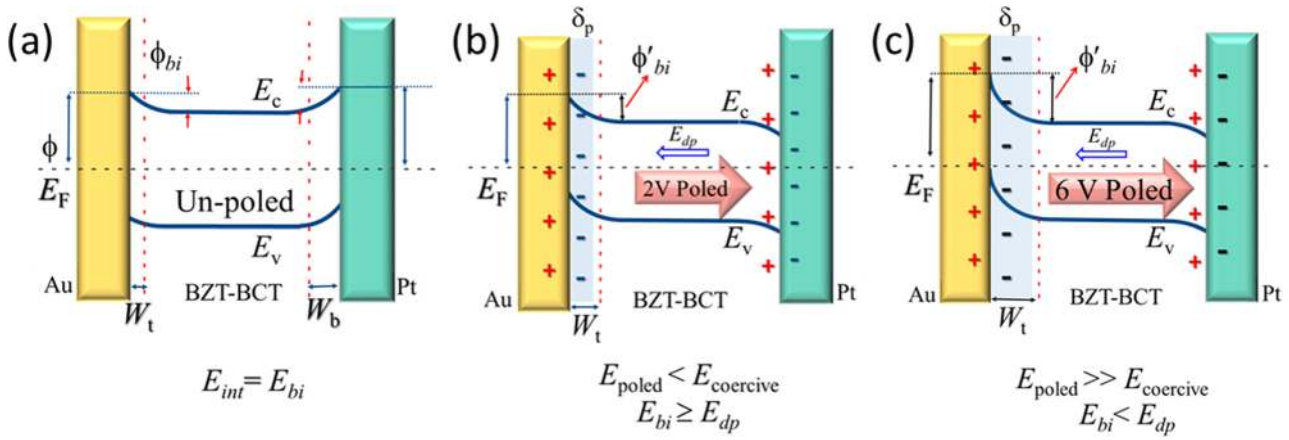

FIG. 4. Schematic energy band diagram showing the variation of the barrier field for (a) un-poled, (b) poled with $E_{poled} < E_{coercive}$, and (c) poled with $E_{poled} > E_{coercive}$ states of the Au/BZT-BCT/Pt film. Here, δ_P is the polarization charge due to poling, and W_t and W_b are the depletion widths at the top and bottom electrode/film interfaces, respectively.

and 4(c), which show the band diagrams for these two cases, i.e., $E_{poled} < E_{coercive}$ and $E_{poled} > E_{coercive}$, respectively. Note that for $E_{poled} > E_{coercive}$, the Schottky barrier width increases largely and hence has as a predominate linear behavior (due to high resistive nature of the width) in a lower bias field and shows the non-linearity at a higher bias field, as depicted in Fig. 2(b).

To give a quantitative picture about the PV mechanism, E_{bi} and E_{dp} are estimated. The estimated φ_t and φ_b based on the work function of Au (5.1 eV), electron affinity (χ_e) of BZT-BCT (3.9 eV) and work function of Pt (6.35 eV) are 1.2 eV and 2.45 eV, respectively. This gives the $E_{bi} \sim 1.7$ MV/m.[35] On the other hand, E_{dp} is calculated from the electrostatic equation $E_{dp} = -\frac{P_r}{\epsilon_0 \epsilon_F}\left(\frac{2\varepsilon_F/d}{2\varepsilon_F/d+\varepsilon_e/\lambda}\right)$,[49,50] where P_r and ε_F are the remnant polarization and dielectric constant of the ferroelectric thin film, respectively. ε_e and λ are the dielectric constant and screening length of the metal electrode, respectively. ε_0 is the permittivity of free space. E_{dp} is calculated at poling fields below and above $E_{coercive}$ using the following values: P_r = 1.44 $\mu C/cm^2$ at 3 V and 4.80 $\mu C/cm^2$ at 8 V. $\varepsilon_F \sim 905$ at 1 kHz (from the dielectric measurement), $\epsilon_e = 2$, and $\lambda = 0.4$ Å(for noble metals such as Au and Pt).[49] The calculated E_{dp} = 0.088 MV/m at 3 V poling ($E_{poled} < E_{coercive}$) is lower than E_{bi} (1.7 MV/m). However, E_{dp} = 2.9 MV/m at 8 V poling ($E_{poled} > E_{coercive}$) is higher than E_{bi}. These values further confirm that the Schottky barrier dominates E_{dp} for sample poled below $E_{coercive}$. However, above $E_{coercive}$, E_{dp} is a major contributing factor for the observed PV response in the BZT-BCT film which is in agreement with the mechanism discussed earlier.

The large photo-response of the BZT-BCT film with sharp ON-OFF transient current characteristics (see the enlarged version of J_{SC} versus time plot in the inset of Fig. 5) under UV-visible light strongly suggests its suitability for self-powered photodetector devices such as the UV detector and visible-blind sensor.[5,35,51] To envisage the photodetector performance, the salient parameters such as the responsivity ($R = I_{ph}/(P \times S)$) and detectivity ($D^* = R/\sqrt{(2eI_{dark}/S)}$), where $I_{ph} = |I_{light}| - |I_{dark}|$, I_{light} is the current in the light ON state, I_{dark} is the current in the light OFF state, P is the incident light intensity, and S is the effective irradiated area, are calculated from the ON and OFF, PV characteristics of the BZT-BCT sample shown in the inset of Fig. 5.[5] The resultant R and D^* values are plotted as a function of poling voltage in Fig. 5. The difference in magnitude, with respect to the polarity of poling voltage, seen in the value of R and D^* is mostly attributed to the asymmetric electrode geometry and its related interface barrier formation. The maximum values of R and D^* observed under the UP-poled state are 2.5×10^{-4} A/W and 2.4×10^9 Jones, respectively. These values are comparable with a BFO system at 100 mW/cm^2 light intensity.[5] Additionally, the switchable, sharp, and stable PV response displayed by the film advocates its application in data storage and logical switching devices, where "electrical writing" and "optical reading" can be performed by poling and light illumination conditions, respectively.[35]

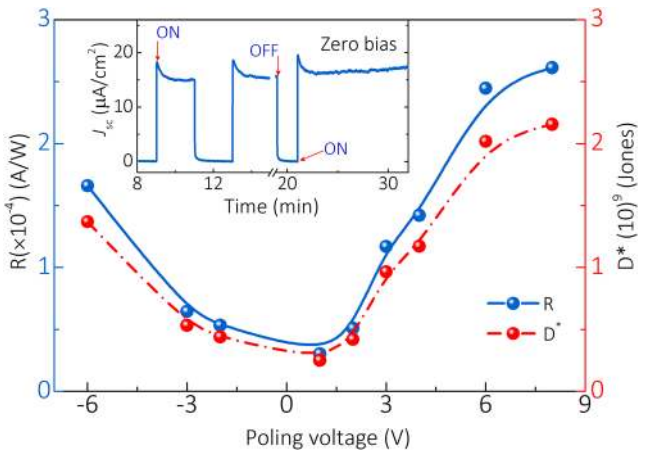

FIG. 5. Calculated *R* and *D** plotted as a function of poling voltage for the BZT-BCT film. The inset is J_{SC} versus time plot under the light ON and OFF state under the zero bias condition.

A good quality polycrystalline Pb-free high piezocoefficient $0.5Ba(Zr_{0.2}Ti_{0.8})O_3$-$0.5(Ba_{0.7}Ca_{0.3})TiO_3$ thin film was fabricated on the $Pt/TiO_2/SiO_2/Si$ substrate by a PLD technique to study the PV characteristics. The structure and crystallinity of the film was confirmed by XRD measurements, and the optical bandgap value of 3.2 eV was deduced from the K-M plot. The observed P-E loop along with the PFM phase and amplitude response to the bias voltage confirms the ferroelectric nature of the film. The studies revealed a large PV response with a maximum of 0.81 V and 36 $\mu A/cm^2$ as V_{OC} and J_{SC}, respectively. Interestingly, the PV studies unveil distinctly different J-V curves at two different poling field regions. The features were well explained in terms of the interfacial barrier formation and its modulation by the polarization induced depolarization field, using the band diagram. Overall, the study demonstrated that the polarization contribution to the PV response was predominant over the interfacial Schottky contribution in the BZT-BCT film poled at above coercive field. Moreover, the calculated photodetector parameters, responsivity and detectivity, strongly suggested the application potentials of the BZT-BCT film in photodetector devices.

REFERENCES

[1] C. Paillard, X. Bai, I. C. Infante, M. Guennou, G. Geneste, M. Alexe, J. Kreisel, and B. Dkhil, Adv. Mater. **28**, 5153 (2016).
[2] Y. Yuan, Z. Xiao, B. Yang, and J. Huang, J. Mater. Chem. A **2**, 6027 (2014).
[3] K. T. Butler, J. M. Frost, and A. Walsh, Energy Environ. Sci. **8**, 838 (2015).
[4] P. Lopez-Varo, L. Bertoluzzi, J. Bisquert, M. Alexe, M. Coll, J. Huang, J. A. Jimenez-Tejada, T. Kirchartz, R. Nechache, F. Rosei, and Y. Yuan, Phys. Rep. **653**, 1 (2016).
[5] J. Qi, N. Ma, X. Ma, R. Adelung, and Y. Yang, ACS Appl. Mater. Interfaces **10**, 13712 (2018).
[6] V. M. Fridkin and B. N. Popov, Sov. Phys. Usp. **126**, 657 (1978).
[7] W. T. H. Koch, R. Munser, W. Ruppel, and P. Würfel, Solid State Commun. **17**, 847 (1975).
[8] W. T. H. Koch, R. Munser, W. Ruppel, and P. Würfel, Ferroelectrics **13**, 305 (1976).
[9] P. Poosanaas and K. Uchino, Mater. Chem. Phys. **61**, 36 (1999).

[10]K. Uchino, Y. Miyazawa, and S. Nomura, Jpn. J. Appl. Phys. **21**, 1671 (1982).
[11]S. Y. Yang, J. Seidel, S. J. Byrnes, P. Shafer, C. H. Yang, M. D. Rossell, P. Yu, Y. H. Chu, J. F. Scott, J. W. Ager, L. W. Martin, and R. Ramesh, Nat. Nanotechnol. **5**, 143 (2010).
[12]L. You, F. Zheng, L. Fang, Y. Zhou, L. Z. Tan, Z. Zhang, G. Ma, D. Schmidt, A. Rusydi, L. Wang, L. Chang, A. M. Rappe, and J. Wang, Sci. Adv. **4**, eaat3438 (2018).
[13]T. Choi, S. Lee, Y. J. Choi, V. Kiryukhin, and S. W. Cheong, Science **324**, 63 (2009).
[14]W. Dong, Y. Guo, B. Guo, H. Li, H. Liu, and T. W. Joel, ACS Appl. Mater. Interfaces **5**, 6925 (2013).
[15]M. Yang, A. Bhatnagar, and M. Alexe, Adv. Funct. Mater. **1**, 1500139 (2015).
[16]D. J. Kim and M. Alexe, Appl. Phys. Lett. **110**, 183902 (2017).
[17]X. Yang, X. Su, M. Shen, F. Zheng, Y. Xin, L. Zhang, M. Hua, Y. Chen, and V. G. Harris, Adv. Mater. **24**, 1202 (2012).
[18]L. Pintilie, I. Vrejoiu, G. L. Rhun, and M. Alexe, J. Appl. Phys. **101**, 064109 (2007).
[19]L. Pintilie, V. Stancu, E. Vasile, and I. Pintilie, J. Appl. Phys. **107**, 114111 (2010).
[20]L. Pintilie, C. Dragoi, and I. Pintilie, J. Appl. Phys. **110**, 044105 (2011).
[21]A. M. Glass, D. Von Der Linde, and T. J. Negran, Appl. Phys. Lett. **25**, 233 (1974).
[22]S. Pal, A. B. Swain, P. P. Biswas, D. Murali, A. Pal, B. R. K. Nanda, and P. Murugavel, Sci. Rep. **8**, 8005 (2018).
[23]M. A. Jalaja and S. Dutta, Adv. Mater. Lett. **6**, 568 (2015).
[24]L. Z. Tan, F. Zheng, S. M. Young, F. Wang, S. Liu, and A. M. Rappe, npj Comput. Mater. **2**, 16026 (2016).
[25]J. E. Spanier, V. M. Fridkin, A. M. Rappe, A. R. Akbashev, A. Polemi, Y. Qi, Z. Gu, S. M. Young, C. J. Hawley, D. Imbrenda, G. Xiao, A. L. Bennett-Jackson, and C. L. Johnson, Nat. Photonics **10**, 611 (2016).
[26]A. Zenkevich, Y. Matveyev, K. Maksimova, R. Gaynutdinov, A. Tolstikhina, and V. Fridkin, Phys. Rev. B **90**, 161409 (2014).
[27]S. M. Young and A. M. Rappe, Phys. Rev. Lett. **109**, 116601 (2012).
[28]D. Lee, S. H. Baek, T. H. Kim, J. G. Yoon, C. M. Folkman, C. B. Eom, and T. W. Noh, Phys. Rev. B **84**, 125305 (2011).
[29]A. Bhatnagar, A. Roy Chaudhuri, Y. Heon Kim, D. Hesse, and M. Alexe, Nat. Commun. **4**, 2835 (2013).
[30]L. Pintilie and M. Alexe, J. Appl. Phys. **98**, 124103 (2005).
[31]J. K. Li, C. Ge, K. J. Jin, J. Y. Du, J. T. Yang, H. Bin Lu, and G. Z. Yang, Appl. Phys. Lett. **110**, 142901 (2017).
[32]J. Zou, Q. Zhang, K. Huang, and N. Marzari, J. Phys. Chem. C **114**, 10725 (2010).
[33]X. Fang, Y. Bando, M. Liao, T. Zhai, U. K. Gautam, A. Li, Y. Koide, and D. Golberg, Adv. Funct. Mater. **20**, 500 (2010).
[34]H. Chen, L. Hu, X. Fang, and L. Wu, Adv. Funct. Mater. **22**, 1229 (2012).
[35]Z. Lu, P. Li, J. G. Wan, Z. Huang, G. Tian, D. Pan, Z. Fan, X. Gao, and J. M. Liu, ACS Appl. Mater. Interfaces **9**, 27284 (2017).
[36]W. Liu and X. Ren, Phys. Rev. Lett. **103**, 257602 (2009).
[37]Z. Sun, C. Ma, M. Liu, J. Cui, L. Lu, J. Lu, X. Lou, L. Jin, H. Wang, and C. L. Jia, Adv. Mater. **29**, 1604427 (2017).
[38]B. Asbani, J.-L. Dellis, A. Lahmar, M. Courty, M. Amjoud, Y. Gagou, K. Djellab, D. Mezzane, Z. Kutnjak, and M. El Marssi, Appl. Phys. Lett. **106**, 042902 (2015).
[39]A. D. Dupuy, Y. Kodera, and J. E. Garay, Adv. Mater. **28**, 7970 (2016).
[40]F. Wang and A. M. Rappe, Phys. Rev. B **91**, 165124 (2015).
[41]F. Z. Li, H. W. Zheng, M. S. Zhu, X. A. Zhang, G. L. Yuan, Z. S. Xie, X. H. Li, G. T. Yue, and W. F. Zhang, J. Mater. Chem. C **5**, 10615 (2017).
[42]P. P. Biswas, T. Chinthakuntla, D. Duraisamy, G. Nambi Venkatesan, S. Venkatachalam, and P. Murugavel, Appl. Phys. Lett. **110**, 192906 (2017).
[43]H. S. Kim, C. R. Lee, J. H. Im, K. B. Lee, T. Moehl, A. Marchioro, S. J. Moon, R. Humphry-Baker, J. H. Yum, J. E. Moser, M. Grätzel, and N. G. Park, Sci. Rep. **2**, 591 (2012).
[44]S. M. Sze and K. K. Ng, *Semiconductor Devices: Physics and Technology*, 3rd ed. (Wiley, New York, 2012).
[45]C. Wang, K. J. Jin, Z. T. Xu, L. Wang, C. Ge, H. B Lu, H. Z. Guo, M. He, and G. Z. Yang, Appl. Phys. Lett. **98**, 192901 (2011).
[46]Z. Xi, J. Ruan, C. Li, C. Zheng, Z. Wen, J. Dai, A. Li, and D. Wu, Nat. Commun. **8**, 15217 (2017).
[47]Z. Tan, J. Tian, Z. Fan, Z. Lu, L. Zhang *et al.*, Appl. Phys. Lett. **112**, 152905 (2018).
[48]K. C. Kao, *Dielectric Phenomena in Solids: with Emphasis on Physical Concepts of Electronic Processes* (Elsevier Academic Press, 2004).
[49]D. J. Kim, J. Y. Jo, Y. S. Kim, Y. J. Chang, J. S. Lee, J. G. Yoon, T. K. Song, and T. W. Noh, Phys. Rev. Lett. **95**, 237602 (2005).
[50]R. R. Mehta, B. D. Silverman, and J. T. Jacobs, J. Appl. Phys. **44**, 3379 (1973).
[51]N. Ma, K. Zhang, and Y. Yang, Adv. Mater. **29**, 1703694 (2017).